This is an *Accepted Manuscript*, which has been through the Royal Society of Chemistry peer review process and has been accepted for publication.

Accepted Manuscripts are published online shortly after acceptance, before technical editing, formatting and proof reading. Using this free service, authors can make their results available to the community, in citable form, before we publish the edited article. We will replace this *Accepted Manuscript* with the edited and formatted *Advance Article* as soon as it is available.

You can find more information about *Accepted Manuscripts* in the **Information for Authors**.

Journal Name

ARTICLE

Efficiency of [2+2] photodimerization of various stilbene derivatives within the DNA duplex scaffold

Tetsuya Doi, Hiromu Kashida* and Hiroyuki Asanuma*

A DNA duplex was used as a scaffold to evaluate intrinsic reactivity of [2+2] photodimerization between stilbene derivatives; the duplex pre-organizes the substrates avoiding the need for an association step. Unmodified stilbenes were first introduced at base-pairing positions on complementary DNA strands. The duplex was then irradiated with 340 nm UV light. HPLC analyses revealed that [2+2] photodimerization proceeded rapidly without side reactions. Thus, it was confirmed that the DNA duplex could be used as an ideal scaffold for [2+2] photodimerization of stilbenes. Next, we examined homo-photodimerization abilities of various stilbene derivatives. Homo-photodimerization of *p*-cyanostilbene, *p*-methylstilbazolium, and *p*-stilbazole occurred efficiently, whereas homo-photodimerization of *p*-dimethylaminostilbene and *p*-nitrostilbene did not proceed at all, probably because the reaction was quenched by dimethylamino and nitro groups. Time-dependent density functional theory calculations revealed that excitation energy was correlated with quantum yield. We further investigated hetero-photodimerization. These reactions were made possible by use of two complementary oligodeoxyribonucleotides tethering different stilbene derivatives. Reactivities in hetero-photodimerization were highly dependent on the combination of derivatives. A high correlation was observed between the quantum yields and energy gaps of HOMO and LUMO between reactive derivatives. Unexpectedly, nitrostilbene, which was non-reactive in homo-photodimerization, cross-reacted with *p*-methylstilbazolium and *p*-stilbazole, both of which had close HOMO or LUMO with nitrostilbene. Evaluation of the intrinsic reactivity of homo- and hetero-photodimerization of stilbene derivatives was made possible by use of DNA as a scaffold.

Introduction

The [2+2] photodimerization of stilbenes has been of interest since Ciamician and Silver characterized dimerization of E-stilbene in 1902.[1] This photodimerization is used for the synthesis of cyclobutane derivatives, in polymer syntheses, and in crosslinking.[2, 3] The effects of concentrations[4] and solvents[5, 6] on photodimerization of stilbenes have been evaluated and reactivities of several stilbene derivatives have been investigated.[7] However, since most photo-cycloadditions are conducted under conditions in which stilbene monomers are dispersed in solvent, molecules must form an aggregate (or a cluster) prior to the photoreaction. Hence, reactivities of stilbene derivatives are dependent on the ability of these derivatives to aggregate. Furthermore, monomeric stilbene also undergoes *trans*-to-*cis* photoisomerization, subsequent cyclization and irreversible phenanthrene formation via oxidation. Accordingly, it was very difficult to distinguish "intrinsic" reactivities from propensity to aggregate. Although clusters have been prepared using nanocages or via attractive interactions[8-14], reactivities remain dependent on dimer aggregate formation. Furthermore, to the best of our knowledge, it has not been possible to evaluate hetero stilbene photodimerization (i.e. cross-reaction between the two different derivatives).

Previously we developed a unique method for preparation of a dye assembly within a DNA duplex.[15, 16] We utilize D-threoninol as a scaffold for the functional molecule, and this residue can be introduced at any position and in any number in an oligodeoxyribonucleotide (ODN) or an oligoribonucleotide using standard solid-phase synthesis techniques. Introduction of the base surrogates at base-pairing positions of complementary strands allows controlled dimer aggregate formation within the duplex. Heterodimers are prepared by hybridizing two strands each of which involves a different dye. We demonstrated that azobenzene dimer formation occurs in an anti-parallel manner scaffolded by ODN duplexes using NMR structural analysis. That the duplex containing dimers or higher order aggregates were unwounded relative to an unmodified duplex was shown by circular dichroism analyses.
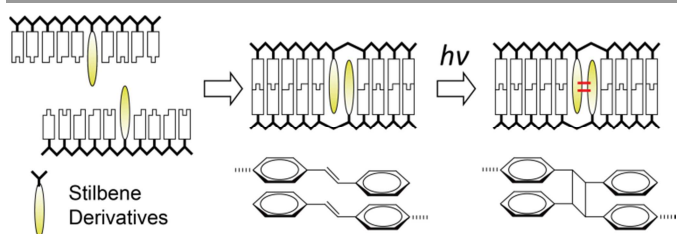
Scheme 1. Schematic illustration of [2+2] photodimerization inside a DNA duplex.

Here, we utilized an ODN duplex as a scaffold for systematic investigation of [2+2] photodimerization between stilbene derivatives whose photoreactivities have not yet been examined in detail. Introduction of stilbene derivatives into base-paring positions of ODNs via D-threoninol allowed us to firmly fix homo- and heterodimer aggregates before photo-irradiation. Upon 340 nm UV irradiation, the [2+2] photodimerization of stilbene derivatives occurs and duplex is crosslinked (Scheme 1). Recently, we examined photodimerization of *p*-stilbazole derivatives to demonstrate that the surrogate via D-threoninol can orthogonally pair with the same surrogate and serve as an artificial base pair for photo-crosslinking of an ODN duplex.[17] We found that photodimerization proceeds very efficiently in the duplex scaffold without other side reactions such as photoisomerization and subsequent cyclization. This result strongly indicates that photodimerization of these surrogates reflects intrinsic reaction ability. In the present study, we investigated the photodimerization of six derivatives in DNA duplexes.
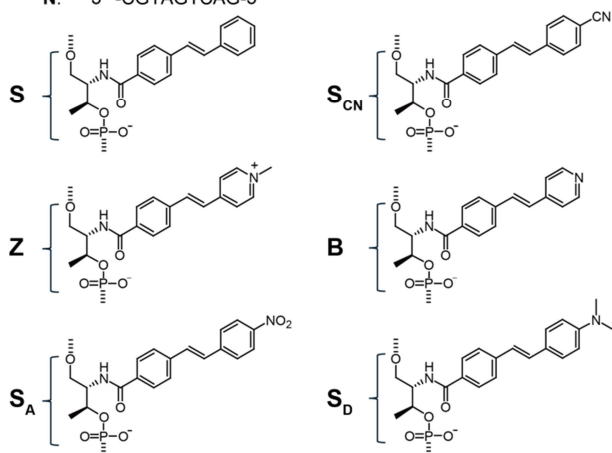

Figure 1. Sequences of ODNs synthesized in this study and chemical structures of stilbene derivatives.

Their intrinsic reactivities in homo- and hetero-photodimerizations were systematically investigated to identify those factors that affect reactivity. We believe that the results reported here complement theoretical investigations[18] and will contribute to better understanding of [2+2] photo-cycloaddition reactions. This strategy will also provide new tools for

photocrosslinking and photoligation that will be used in biotechnology.[19-26]
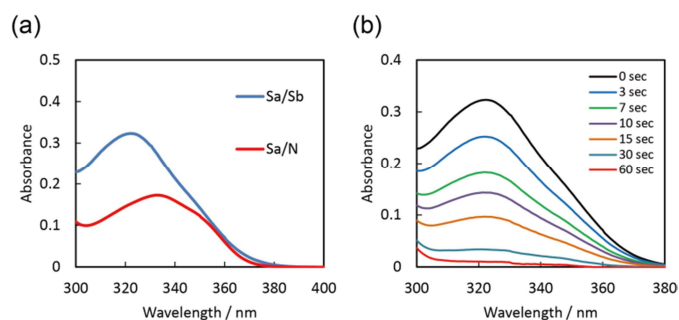
Figure 2. UV-vis spectra of **Sa/Sb** (blue) and **Sa/N** (red). (b) **Sa/Sb** before and after indicated duration of UV irradiation (340 nm). Solution conditions were 5.0 μM DNA, 100 mM NaCl, 10 mM phosphate buffer (pH 7.0), 20 °C.

Results and discussion

Photochemical Properties of Stilbene-Modified ODN and Analysis of [2+2] Photodimerization of Homodimer Aggregate.

Figure 1 show the chemical structures of the six stilbene derivatives studied. In the present study, in addition to the previously reported stilbazole derivatives, *p*-stilbazole (**B**) and *p*-methylstilbazolium (**Z**), we have newly synthesized stilbene (**S**) and *p*-cyanostilbene (**S**$_{CN}$), the stilbene derivatives that are known to dimerize upon UV photo-irradiation. Moreover, we also synthesized *p*-nitrostilbene (**S**$_A$) and *p*-dimethylaminostilbene (**S**$_D$); these derivatives have not been previously characterized. These derivatives were linked to D-threoninols and introduced into an ODN via phosphoramidite chemistry. Sequences of the ODNs are also shown in Figure 1. First, we prepared the homodimer aggregate of unmodified stilbene (**S**) that has been conventionally used for examining photodimerization and investigated its intrinsic reactivity. Figure 2a shows UV-vis spectra of the homo **Sa/Sb** duplex. Before photo-irradiation, **Sa/Sb** had an absorption maximum at 322 nm, which was 13 nm shorter than that of a duplex with a single **S** moiety (**Sa/N**; 335 nm). This hypsochromic shift indicates that **S** moieties in **Sa/Sb** form an H aggregate before photo-irradiation. Similar hypsochromic shifts were observed with all the homodimers examined in this study (Fig. S1), demonstrating all derivatives formed a dimer aggregate scaffolded by the DNA duplex before photo-irradiation. The absorption band rapidly decreased as a function of irradiation time, and after 1 min, the absorption band of **S** had completely disappeared (Fig. 2b). This disappearance of the π-π* band strongly indicated that the [2+2] photodimerization occurred between the two stilbene residues.

The photodimerization reaction was further analyzed by HPLC (Fig. 3). Before photo-irradiation, two peaks that corresponded to the single-stranded **Sa** and **Sb** were observed. After 3 min irradiation, the two peaks completely disappeared and a new single peak appeared at a shorter retention time. MALDI-TOF MS analysis confirmed that this new peak was a crosslinked **Sa/Sb** duplex (Fig. S2). This result unambiguously

demonstrates that the duplex was crosslinked via [2+2] photodimerization of **S** without any side photoreaction. The peak may involve two diastereomers, derived from rotation of stilbenes as we previously reported.[17]
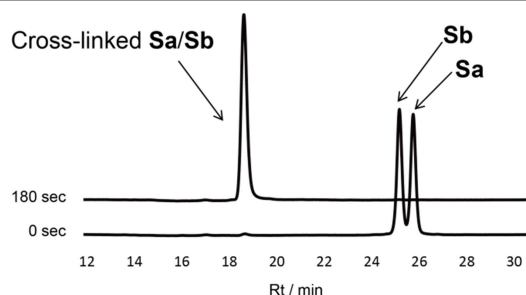
Figure 3. HPLC chromatograms of **Sa/Sb** under conditions that denature the duplex before and after 180 sec UV photo-irradiation (340 nm).

We also investigated thermal stability of the DNA duplex before and after photodimerization. Before photo-irradiation, the T_m of **Sa/Sb** was 42.4 °C (Fig. S3). And after photo-irradiation, the T_m increased to more than 80 °C, confirming that the duplex is crosslinked. From these results, we concluded that [2+2] photodimerization of stilbene occurred within the ODN duplex scaffold and that *trans*-to-*cis* photoisomerization and subsequent cyclization were completely suppressed.
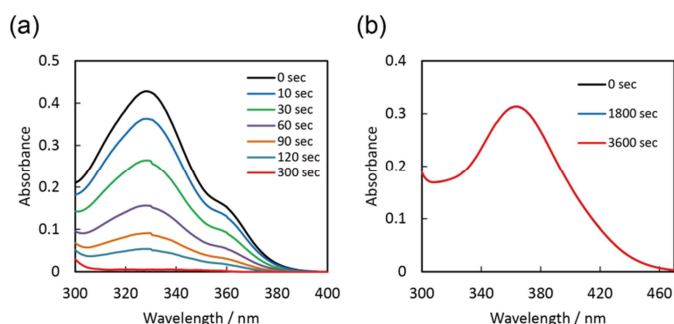
Figure 4. UV-vis spectra of (a) $S_{CN}a/S_{CN}b$ and (b) $S_A a/S_A b$ before and after indicated duration of UV irradiation (340 nm). Solution conditions were 5.0 µM DNA, 100 mM NaCl, 10 mM phosphate buffer (pH 7.0), 20 °C. Note that UV spectra in (b) after 0 sec and 1800 sec overlap with that after 3600 sec almost completely.

Photodimerizations of Homodimer Aggregates of *p*-Cyanostilbene and *p*-Nitrostilbene.

Next, we investigated [2+2] homo-photodimerization of stilbene derivatives S_{CN} and S_A with electron-withdrawing substituents. The UV-vis spectra of the duplexes tethering these moieties, $S_{CN}a/S_{CN}b$ and $S_A a/S_A b$, are shown in Fig. 4. Before photo-irradiation, absorption maximum at 329 nm and 364 nm were observed for S_{CN} and S_A, respectively. Upon photo-irradiation of $S_{CN}a/S_{CN}b$, the band at 329 nm rapidly decreased and the band completely disappeared after 5 min of irradiation (Fig. 4a), which indicates that [2+2] photodimerization of S_{CN} occurred. This photodimerization was further confirmed by HPLC and MALDI-TOF (Figs. S4, S5). In contrast, photo-

irradiation of $S_A a/S_A b$ did not cause any change in the spectrum (Fig. 4b), indicating that *p*-nitrostilbene did not photodimerize.

Photodimerization of *p*-Dimethylaminostilbene.

We then investigated photodimerization of a stilbene derivative modified with an electron donating group, S_D; the photodimerization behavior of this derivative has not been previously analyzed. The pK_a of the dimethylamino group of S_D is around 7; therefore, we investigated the photodimerization of S_D in both deprotonated (pH 9) and protonated (pH 5) states. At pH 9, the absorption maximum appeared at 370 nm, and the peak shifted to 321 nm at pH 5 due to deconjugation resulting from protonation of the dimethylamino group. After 5 min of 340 nm irradiation of $S_D a/S_D b$ at pH 9, no change was observed in the band (Fig. 5a), demonstrating that *p*-dimethylaminostilbene, like *p*-nitrostilbene, did not photodimerize. In striking contrast, when the protonated $S_D a/S_D b$ duplex (pH 5) was irradiated, the band at 321 nm rapidly decreased (Fig. 5b). Photodimerization was also confirmed by HPLC and MALDI-TOF MS analyses; no undesired photoreaction products were observed (Figs. S6, S7). Thus, *p*-dimethylaminostilbene does not undergo [2+2] photodimerization in the deprotonated state but efficiently photodimerizes in protonated state.
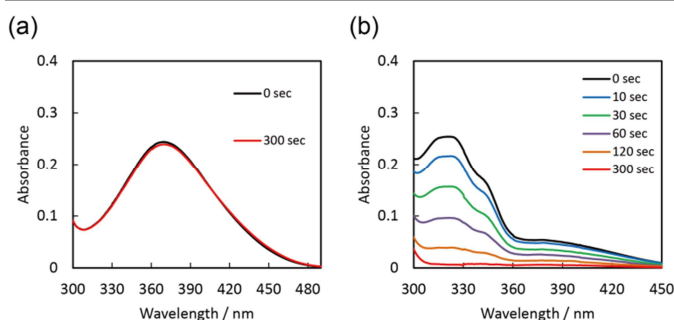
Figure 5. UV-vis spectra of (a) $S_D a/S_D b$ at pH 9.0 (10 mM Tris buffer) and (b) $S_D a/S_D b$ at pH 5.0 (10 mM MES buffer) before and after indicated duration of UV irradiation (340 nm). Solution conditions were 5.0 µM DNA, 100 mM NaCl, 20 °C.

Quantitative Comparison of the Reactivities of Homodimer Aggregates by Quantum Yield

In order to compare intrinsic reactivities of these stilbene derivatives quantitatively, we evaluated quantum yields of homo-photodimerization by using the chemical actinometry method (Fig. 6 and Table 1). Quantum yields of *p*-methylstilbazolium (**Z**) and *p*-stilbazole (**B**) are also shown. Among the six stilbene derivatives, unsubstituted stilbene showed the highest quantum yield, $\Phi = 0.15$. This quantum yield was lower than that of stilbene monomer in benzene solution reported previously ($\Phi = 0.33$)[4]. The lowered quantum yield in the duplex may be attributed to the difference of the solvents or to the quenching by adjacent nucleotides (*vide infra*). Protonated S_D (**H$^+$**) showed the second highest quantum yield (0.036); **B**, **Z**, and S_{CN} showed almost the same quantum yields (0.024, 0.017 and 0.022, respectively). In contrast,

Table 1. Photochemical properties and quantum yields of homodimers of stilbene derivatives.

Sequence	λ_{max}/nm^a	$T_m/°C^b$	HOMO/eV^c	LUMO/eV^c	$\Delta E/eV^{c,d}$	Φ (*10^2)
Sa/Sb	322	42.4	-6.05	-1.72	4.33	15
S$_{CN}$a/S$_{CN}$b	329	53.8	-6.28	-2.16	4.12	2.2
Za/Zb	342	51.5	-6.81	-2.98	3.83	1.7
Ba/Bb	322	46.4	-6.39	-1.99	4.40	2.4
S$_D$a/S$_D$b(H+)^e	321	37.5	-6.33	-2.05	4.28	3.6
S$_D$a/S$_D$b^f	370	36.7	-5.17	-1.51	3.66	N/A
S$_A$a/S$_A$b	364	58.1	-6.37	-2.61	3.76	N/A

^{a}Absorption maximum in UV-vis spectrum. ^{b}Melting temperature of duplex before photo-irradiation. ^{c}TD-DFT calculation values from pbe1pbe/6-31G*, solvent: water. ^{d}Difference in energies between LUMO and HOMO. ^{e}Measured at pH 5. ^{f}Measured at pH 9.

homodimer aggregates of both **S$_A$** and **S$_D$** did not undergo photodimerization reaction at all; their quantum yields were nil. Thus, quantum yields of homo-photodimerization are highly dependent on substituents.

In order to elucidate the factors that determine reactivities of homo-photodimerization of stilbene derivatives, we measured or calculated several photochemical properties, which are listed in Table 1. There was no correlation between quantum yields and T_ms of duplexes. For instance, **S$_{CN}$a/S$_{CN}$b** had a higher T_m (53.8 °C) than **Sa/Sb** (42.4 °C), likely due to facilitated stacking interaction by the electron-withdrawing cyano group; however, the quantum yield of **S$_{CN}$a/S$_{CN}$b** was far lower than that of **Sa/Sb**. Since the photodimerization reaction was conducted at 20 °C, T_m may not affect the reaction as all duplexes should have been stable at this temperature. Interestingly, however, we did observe a distinct correlation between quantum yield and excitation energy (ΔE = LUMO-HOMO); the derivatives with higher ΔE showed higher quantum yields, except for **S$_A$** and **S$_D$** (*vide infra*). For example, the **S** moiety, which had the highest quantum yield of derivatives evaluated, also had among the highest ΔE values. Caldwell predicted that high singlet energies are favorable for photodimerization.[18, 27] Our experimental results agree with this prediction except for derivative **B**: the quantum yield of **Ba/Bb** was lower than that of **Sa/Sb**, whereas its ΔE was higher than that of **S**. Protonation of pyridine ring of **B** at pH 7 may affect the photodimerization efficiency.[28]

As we noted above, quantum yield of photodimerization of unmodified stilbene in the duplex was lower than that in the benzene solution. We hypothesize that the lower efficiency in the duplex is due to quenching by the adjacent bases as quenching of fluorophores by electron transfer from nucleobases, especially guanine, has been previously observed.[29] In order to investigate effects of the base neighboring the stilbene derivatives, ODNs tethering **S**, **B**, and **Z** moieties flanked by AT pairs were synthesized. The quantum yields for these modified duplexes were higher than those from duplexes with GC pairs neighboring the stilbene derivatives (Table S1), indicating that neighboring guanine quenched the excited state and inhibited the photodimerization. Though this quenching might affect the photochemical reaction in DNA duplex, quantum yields remained in the same order (**S** > **B** > **Z**), irrespective of neighboring nucleobase. So, we concluded that the qualitative analysis of the photoreactivities was not affected by the flanking native base pairs.

S$_A$ and **S$_D$** did not undergo photodimerization within the DNA duplex scaffold, which can be explained by quenching of the excited state by nitro and dimethylamino substituent groups.[30] In the case of **S$_D$**, an electron on the dimethylamino group would be intramolecularly transferred to form an intramolecular charge transfer state after photo excitation, and this would suppress the dimerization reaction. Intramolecular electron transfer quenches fluorescence of dyes substituted with the dimethylamino group.[31] Consistently, protonation of dimethylamino group (**S$_D$(H$^+$)**, see Fig. 6) allowed photodimerization (quantum yield increased from nil to 0.036), which strongly supports our hypothesis.

According to Rullière et al., photo-excited 4-dimethylamino-4'-nitrostilbene undergoes fast rotation of nitro group, which facilitates non-radiative decay of excited state.[32] In the case of **S$_A$**, which has a nitro group at the *para*-position, similar fast rotation of nitro group likely resulted in non-radiative decay from an excited state and suppressed photodimerization. For other stilbene derivatives, quantum yields of photodimerization correlated strongly with ΔE values, although further theoretical investigations are required to validate the proposed mechanism.
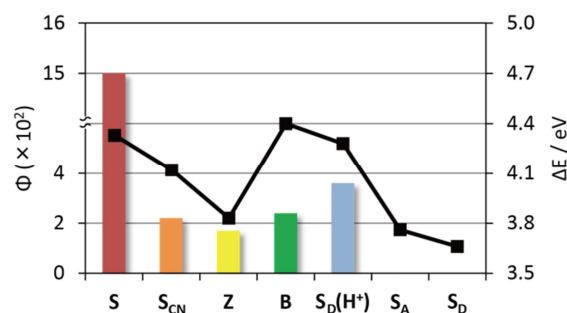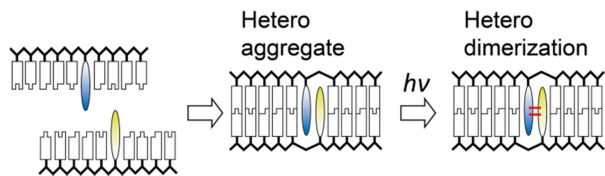

Figure 6. Quantum yields of homo-photodimerizations (bar graph) and calculated excitation energies (line graph). $\Delta E = E_{LUMO} - E_{HOMO}$.

Cross-photodimerizations of Heterodimer Aggregates.

Next, we investigated hetero [2+2] photodimerization, that is, photodimerization between different stilbene derivatives, using the DNA duplex as a scaffold to place different derivatives in proximity (Scheme 2). Cross-photoreactivity between the different stilbene derivatives has not yet been reported due to the difficulty in preparing the pre-organized heterodimer aggregate. With our ODN strategy, heterodimer aggregates can be easily prepared by hybridization of complementary DNA

strands tethering different dyes. Here, reactivities of hetero [2+2] photodimerization of combinations of the six stilbene derivatives were systematically investigated by combining two complementary ODNs, each of which tethered a different stilbene derivative. We monitored photodimerization between different derivatives using UV-vis spectroscopy upon 340 nm UV irradiation (Figs. S10-S16); calculated quantum yields are summarized in Table 2.

Scheme 2. Schematic illustration of hetero [2+2] photodimerization using DNA duplex as a scaffold.

Table 2. Quantum yields of homo- and hetero-photodimerizations.

| Y \ X	$\Phi(\times 10^2)$						
	S	**S_{CN}**	**Z**	**B**	**S_A**	**S_D**[a]	**$S_D(H^+)$**[b]
S	15	7.9	0.08	2.4	N/A	N/A	6.0
S_{CN}	8.9	2.2	0.89	2.0	N/A	N/A	2.8
Z	N/A	0.14	1.7	1.4	0.02	N/A	0.18
B	2.8	1.3	1.6	2.4	0.01	N/A	0.28
S_A	N/A	N/A	0.08	0.04	N/A	N/A	N/A
S_D[a]	N/A	N/A	N/A	N/A	N/A	N/A	-
$S_D(H^+)$[b]	4.5	1.1	0.36	0.31	N/A	-	3.6

[a]Measured at pH 9. [b]Measured at pH 5.

Cross-photodimerization among the Reactive Derivatives.

Cross-dimerization proceeded for all combinations of "reactive" derivatives (**S**, **S_{CN}**, **B**, **Z**, **$S_D(H+)$**), although their reactivities significantly depended on the counterpart. For instance, reactivity with **S** was in the order of **S/S** > **S/S_{CN}** > **S/$S_D(H^+)$** > **S/B** > **S/Z** (see first column and first row of Table 2). Interestingly, the order was completely different in the series of **Z** combination: The order of reactivity was **Z/Z** > **Z/B** > **Z/S_{CN}** > **Z/$S_D(H^+)$** > **Z/S**. This tendency was entirely different from the reactivities in homo combinations, in which **S/S** showed the highest reactivity (Table 2). The reactivity order of photodimerizaton was highly correlated with the energy gap of the frontier orbitals between the derivatives but was not correlated with T_ms (Table S2). Figure 7a shows the quantum yields of photodimerizations and energy gaps of frontier molecular orbitals between **S** and each derivative (ΔHOMO or ΔLUMO). There were significant correlations between the quantum yields and ΔHOMO and ΔLUMO. The **S/S** homo combination with no energy gap showed the highest quantum yield, whereas the **S/Z** pair with the largest energy gap showed the smallest quantum yield. Similar trends were also observed in the reactivities of **S_{CN}** combination as shown in Fig. 7b. Except for the **S_{CN}/S** combination, lower energy gaps were

correlated with higher cross-reactivities. The relatively high reactivity of **S** may result from a high excitation energy of **S** or from less electron transfer from native nucleobases to this derivative.

In striking contrast to **S** and **S_{CN}**, **Z** showed the lowest quantum yield with **S**, although **S** showed the highest reactivity among homo combinations (Figure 7c). **Z** showed the highest quantum yield with **Z** in complementary strand. The reactivities of **Z** also correlated with energy gaps. Derivatives **B** and **$S_D(H+)$** showed similar correlations between quantum yields and energy gaps (Figs. S17, S18). These results strongly indicate that the energy gap between the two stilbene derivatives is an important factor determining reactivity of heterodimerizations. Small energy gap is favorable for effective photodimerization, and *vice versa*.
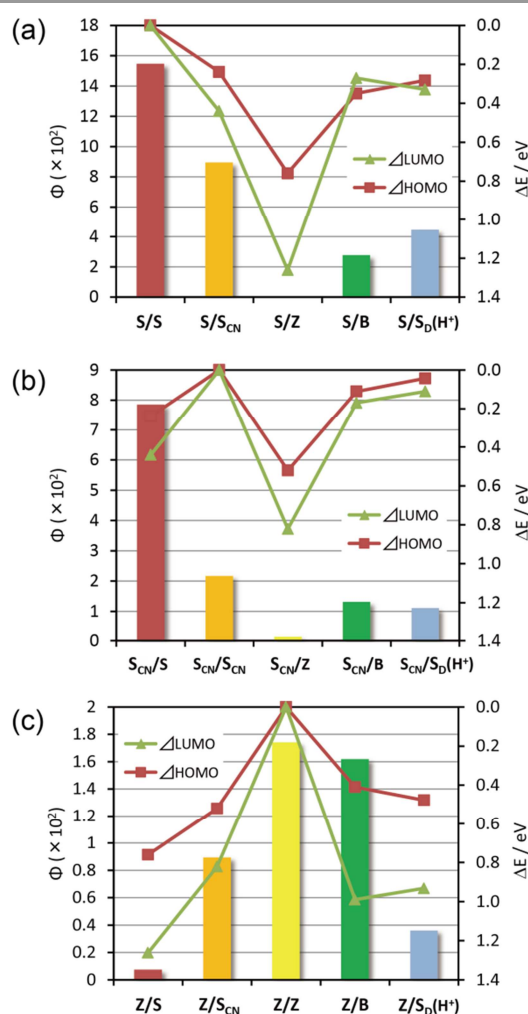

Figure 7. Quantum yields of photodimerizations of (a) **Sa/Yb**, (b) **S_{CN}a/Yb**, (c) **Za/Yb** (**X, Y=S**, **Z**, **S_{CN}** **B**, **$S_D(H^+)$**) duplexes (bar graphs) and energy gaps of HOMO or LUMO (line graphs). The energy gaps are displayed in absolute value and the axis is inverted.

Contributions of these frontier orbitals to the reactivity of photodimerization seem reasonable, because both HOMO and LUMO of each stilbene may interact intermolecularly for [2+2] photodimerizations.[33]

Cross-reactivity of Non-reactive S_A or S_D with Other Reactive Derivatives.

Neither S_A nor S_D underwent homo-photodimerizaiton. Surprisingly, however, both **B** and **Z** cross-reacted with inactive S_A (Fig. 8), although the quantum yield was below 10^{-3} and very small amounts of side products were observed by HPLC (Figs. S19, S20). In contrast, S_D did not cross-react with any of the stilbene derivatives. These cross-reactivities cannot be explained simply by the energy gap of HOMO or LUMO.
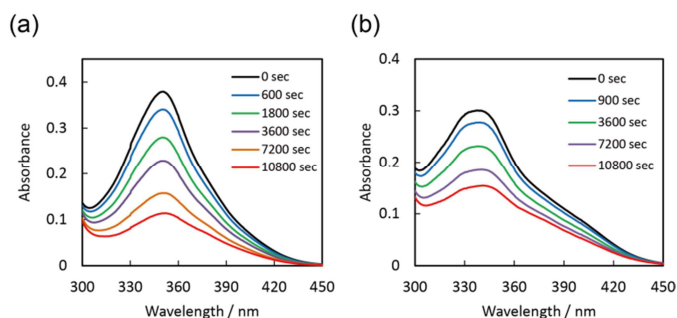
Figure 8. UV-vis spectra of (a) $S_A a/Zb$ and (b) $S_A a/Bb$ before and after indicated duration of UV irradiation (340 nm) time. Solution conditions were 5.0 μM DNA, 100 mM NaCl, 10 mM phosphate buffer (pH 7.0), 20 °C.

Irradiation with 340 nm light excites the stilbene derivative either in strand "a" or "b" in the heterodimer aggregate because all the derivatives absorb at 340 nm. For example, irradiation of X/S_D excites either **X** or S_D, but not both simultaneously, to afford either X^*/S_D or X/S_D^*. In both cases, the excited state should be quenched by inter- or intra-molecular charge transfer from dimethylamino group. Accordingly, the heterodimer aggregate with S_D does not undergo photodimerization irrespective of the energy gap of HOMO or LUMO. But in the case of a S_A heterodimer aggregate, the decay path of X^*/S_A is different from that of X/S_A^*. In the X/S_A^* state, S_A^* should non-radiatively decay in the same manner as it would in a S_A homodimer aggregate; fast rotation of the nitro group will result in non-radiative decay from an excited state and suppressed photodimerization. However, excited X^* in X^*/S_A cannot be quenched by the fast rotation of nitro group. Resonance energy transfer (i.e. the energy transfer from the excited species to the unexcited one) might facilitate rapid migration between X^*/S_A and X/S_A^*, and some of X^*/S_A may be decayed non-radiatively via conversion to X/S_A^*. In the X^*/S_A state, however, formation of the cyclobutane ring can occur. **Z** and **B** were both reactive with S_A because either HOMO or LUMO levels were close; ΔHOMO of B/S_A and ΔLUMO of Z/S_A were 0.02 and 0.37 eV, respectively. Accordingly, **B** and **Z** cross-photodimerized with S_A although their intrinsic reactivities were far smaller than that of **S**.

At present, we cannot propose a clear intermediate or pathway for the photodimerization reactions of these stilbene derivatives. The intermediate electronic state of the radical ion pair as depicted in Fig. S21 is also possible. [34, 35] Theoretical calculations and ultrafast spectroscopic measurements will provide important clues to understanding these interesting phenomena.

Conclusions

We have successfully developed a new methodology to evaluate the [2+2] photodimerization reactivities of various stilbene derivatives by using a DNA duplex as a scaffold. When a duplex tethering a stilbene pair at its center was irradiated with 340 nm UV light, photodimerization occurred rapidly. UV-vis and HPLC analyses revealed that photodimerization proceeded selectively and no side reactions occurred. Protonated *p*-dimethylaminostilbene and *p*-cyanostilbene also dimerized upon photo-irradiation, whereas *p*-nitrostilbene and deprotonated *p*-dimethylaminostilbene were inactive. Time-dependent density functional theory calculations indicated that excitation energy is correlated with efficient homo-photodimerization. Homo-photodimerization of *p*-dimethylaminostilbene and *p*-nitrostilbene probably did not proceed due to quenching by dimethylamino and nitro groups, respectively. We also investigated the reactivity of hetero-dimerization controlled by hybridizing DNA strands tethering different derivatives. The quantum yields of hetero-dimerization showed excellent correlation with the energy gaps of frontier molecular orbitals. Furthermore, we have unexpectedly found that non-reactive nitrostilbene could photodimerize with stilbazole or methylstilbazolium. This observation will lead to further experimental and theoretical mechanistic studies and this strategy should prove useful for photocrosslinking and photoligation in biotechnology applications. Although photocycloadditions are extensively applied in biological fields such as crosslinking of nucleic acids[36, 37], their detailed reactivities between nucleobases and crosslinkers are still not known. Our results on hetero-photodimerization might illustrate their reactivities by focusing on energy gaps of HOMO or LUMO between nucleobases and crosslinkers.

Experimental Section

Materials

All conventional phosphoramidite monomers, CPG columns, and reagents for DNA synthesis were purchased from Glen Research. Other reagents for the syntheses of phosphoramidite monomers were purchased from Tokyo Chemical Industry, Wako, and Aldrich. Unmodified ODNs were purchased from Integrated DNA Technologies.

Synthesis of ODNs

All the modified ODNs were synthesized on an automated DNA synthesizer (H-8-SE, Gene World) by using phosphoramidite monomers bearing **S**, S_{CN}, **Z**, **B**, S_A, or S_D. Syntheses of phosphoramidite monomers **B** and **Z** were reported previously.[17] **S**, S_{CN}, S_A, and S_D were synthesized as described in the Supporting Information. Samples were handled under dark to avoid photoreaction in ambient light. After

workup, ODNs were purified by reversed phase HPLC and characterized using a matrix-assisted laser desorption ionization time-of-flight mass spectrometer (MALDI-TOF; Autoflex II, Bruker Daltonics). MALDI-TOF MS data for the synthesized ODNs: **Sa**, obsd 3071 (calcd for [**Sa** + H$^+$], 3072); **Sb**, obsd 3111 (calcd for [**Sb** + H$^+$], 3111); **S$_{CN}$a**, obsd 3098 (calcd for [**S$_{CN}$a** + H$^+$], 3097); **S$_{CN}$b**, obsd 3137 (calcd for [**S$_{CN}$b** + H$^+$], 3136); **S$_A$a**, obsd 3117 (calcd for [**S$_A$a** + H$^+$], 3116); **S$_A$b**, obsd 3157 (calcd for [**S$_A$b** + H$^+$], 3157); **S$_D$a**, obsd 3114 (calcd for [**S$_D$a** + H$^+$], 3115); **S$_D$b**, obsd 3155 (calcd for [**S$_D$b** + H$^+$], 3155).

Spectroscopic Measurements

UV-vis spectra were measured on a JASCO model V-560 equipped with a programmable temperature controller; 10-mm quartz cells were used.

Measurement of the Melting Temperature

The melting curves were obtained with a Shimadzu UV-1800 by measuring the change in absorbance at 260 nm versus temperature. The melting temperature (T_m) was determined from the maximum in the first derivative of the melting curve. Both the heating and the cooling curves were measured, and the calculated T_ms from these curves agreed to within 2.0 °C. The temperature ramp was 0.5 °C min^{-1}.

Chemical Actinometry

Quantum yields were determined by using 3,4-dimethoxynitrobenzene actinometry as reported by Zhang et al.[38] Conversion rate was calculated from the UV-vis spectra at each irradiation time, and the quantum yields were determined by calculating the ratio between initial slope and absorbed photons determined by actinometry.

UV Irradiation

A xenon light source (MAX-301, Asahi Spectra) equipped with interference filters centered at 340.0 nm (half bandwidth 10 nm, power density 0.15 mW/cm^2) was used for photoreaction. The sample solution was added to a cuvette, and the temperature of light irradiation was controlled using a programmable temperature controller. Photo-irradiation was conducted at 20 °C.

HPLC Analyses

A Merck LiChrospher 100 RP-18(e) column heated to 50 °C was used for HPLC analyses. The flow rate was 0.5 mL/min. A solution of 50 mM ammonium formate (solution A) and a mixture of 50 mM ammonium formate and acetonitrile (50/50, v/v; solution B) were used as mobile phases. A linear gradient of 5–35% solution B over 30 min was employed. HPLC chromatograms were monitored at 260 nm.

Acknowledgements

Notes and References

Graduate School of Engineering, Nagoya University, Furo-cho, Chikusa-ku, Nagoya, 464-8603, Japan. E-mail: asanuma@nubio.nagoya-u.ac.jp, kashida@nubio.nagoya-u.ac.jp; Fax: +81 52 789 2528; Tel: +81 52 789 2488

1. G. Ciamician and P. Silber, *Chem. Ber.*, 1902, **35**, 4128-4131.
2. M. Schraub, H. Gray and N. Hampp, *Macromolecules*, 2011, **44**, 8755-8762.
3. G. W. Goodall and W. Hayes, *Chem. Soc. Rev.*, 2006, **35**, 280-312.
4. F. D. Lewis and D. E. Johnson, *J. Photochem.*, 1977, **7**, 421-423.
5. M. S. Syamala and V. Ramamurthy, *J. Org. Chem.*, 1986, **51**, 3712-3715.
6. Y. Ito, T. Kajita, K. Kunimoto and T. Matsuura, *J. Org. Chem.*, 1989, **54**, 587-591.
7. H. Ulrich, D. V. Rao, F. A. Stuber and A. A. R. Sayigh, *J. Org. Chem.*, 1970, **35**, 1121-1125.
8. S. Yamada, N. Uematsu and K. Yamashita, *J. Am. Chem. Soc.*, 2007, **129**, 12100-12101.
9. A. Papagni, P. D. Buttero, C. Bertarelli, L. Miozzo, M. Moret, M. T. Pryce and S. Rizzato, *New J. Chem.*, 2010, **34**, 2612-2621.
10. W. Herrmann, S. Wehrle and G. Wenz, *Chem. Commun.*, 1997, 1709-1710.
11. K. S. S. P. Rao, S. M. Hubig, J. N. Moorthy and J. K. Kochi, *J. Org. Chem.*, 1999, **64**, 8098-8104.
12. R. Kaliappan, L. S. Kaanumalle, A. Natarajan and V. Ramamurthy, *Photochem. Photobiol. Sci.*, 2006, **5**, 925-930.
13. M. Pattabiraman, A. Natarajan, R. Kaliappan, J. T. Mague and V. Ramamurthy, *Chem. Commun.*, 2005, 4542-4544.
14. M. V. S. N. Maddipatla, L. S. Kaanumalle, A. Natarajan, M. Pattabiraman and V. Ramamurthy, *Langmuir*, 2007, **23**, 7545-7554.
15. H. Kashida, T. Fujii and H. Asanuma, *Org. Biomol. Chem.*, 2008, **6**, 2892-2899.
16. T. Fujii, H. Kashida and H. Asanuma, *Chem. Eur. J.*, 2009, **15**, 10092-10102.
17. H. Kashida, T. Doi, T. Sakakibara, T. Hayashi and H. Asanuma, *J. Am. Chem. Soc.*, 2013, **135**, 7960-7966.
18. R. A. Caldwell, *J. Am. Chem. Soc.*, 1980, **102**, 4004-4007.
19. F. D. Lewis, T. Wu, E. L. Burch, D. M. Bassani, J.-S. Yang, S. Schneider, W. Jaeger and R. L. Letsinger, *J. Am. Chem. Soc.*, 1995, **117**, 8785-8792.
20. K. Fujimoto, S. Matsuda, N. Takahashi and I. Saito, *J. Am. Chem. Soc.*, 2000, **122**, 5646-5647.
21. S. Ogasawara and K. Fujimoto, *Angew. Chem. Int. Ed.*, 2006, **45**, 4512-4515.

22. T. Ihara, T. Fujii, M. Mukae, Y. Kitamura and A. Jyo, *J. Am. Chem. Soc.*, 2004, **126**, 8880-8881.

23. J. Manchester, D. M. Bassani, J.-L. H. A. Duprey, L. Giordano, J. S. Vyle, Z. Zhao and J. H. R. Tucker, *J. Am. Chem. Soc.*, 2012, **134**, 10791-10794.

24. M. Mukae, T. Ihara, M. Tabara and A. Jyo, *Org. Biomol. Chem.*, 2009, **7**, 1349-1354.

25. K. Pasternak, A. Pasternak, P. Gupta, R. N. Veedu and J. Wengel, *Bioorg. Med. Chem.*, 2011, **19**, 7407-7415.

26. K. Fujimoto, A. Yamada, Y. Yoshimura, T. Tsukaguchi and T. Sakamoto, *J. Am. Chem. Soc.*, 2013, **135**, 16161-16167.

27. We also investigated the correlation between the energy level of HOMO or LUMO. See **Fig.S8** for details. It also showed a good correlation and we could not determine critical factor determining the reactivities in homo combination.

28. We also measured the photodimerization of **B** at pH 9. As shown in **Fig.S9**, the reactivity was enhanced which indicates that the protonation has suppressed the reaction.

29. M. Torimura, S. Kurata, K. Yamada, T. Yokomaku, Y. Kamagata, T. Kanagawa and R. Kurane, *Anal. Sci.*, 2001, **17**, 155-160.

30. Orientation of double bond should affect the reactivities. In UV-VIS spectra, all derivatives showed hypsochromic shift, demonstrating they formed H-type aggregate in DNA duplexes. In addition, no correlation was observed between melting temperatures and quantum yields, indicating strength of stacking interaction did not significantly affect the reactivities. Hence, we believe effects of the difference of the orientation on the photodimerization reactivities are marginal.

31. A. P. de Silva, H. Q. N. Gunaratne, T. Gunnlaugsson, A. J. M. Huxley, C. P. McCoy, J. T. Rademacher and T. E. Rice, *Chem. Rev.*, 1997, **97**, 1515-1566.

32. J. Oberlé, E. Abraham, G. Jonusauskas and C. Rullière, *J. Raman Spectrosc.*, 2000, **31**, 311-317.

33. I. Fleming, *Frontier Orbitals and Organic Chemical Reactions*, Wiley, NewYork, 1976.

34. K. S. Peters, S. C. Freilich and J. Lee, *J. Phys. Chem.*, 1993, **97**, 5482-5485.

35. K. S. Peters and J. Lee, *J. Phys. Chem.*, 1992, **96**, 8941-8945.

36. A. Shigeno, T. Sakamoto, Y. Yoshimura and K. Fujimoto, *Org. Biomol. Chem.*, 2012, **10**, 7820-7825.

37. M. Grigoriev, D. Praseuth, A. L. Guieysse, P. Robin, N. T. Thuong, C. Hélène and A. Harel-Bellan, *Proc. Natl. Acad. Sci. USA*, 1993, **90**, 3501-3505.

38. J.-Y. Zhang, H. Esrom and I. W. Boyd, *Appl. Surf. Sci.*, 1999, **138–139**, 315-319.